

Stability and multistability of synchronization in networks of coupled phase oscillators

Yun Zhai(翟云), Xuan Wang(王璇), Jinghua Xiao(肖井华), and Zhigang Zheng(郑志刚)

Citation: Chin. Phys. B, 2023, 32 (**6**): 060503. DOI: 10.1088/1674-1056/acc808
Journal homepage: http://cpb.iphy.ac.cn; http://iopscience.iop.org/cpb

What follows is a list of articles you may be interested in

Synchronization of stochastic complex networks with time-delayed coupling

Duolan(朵兰), Linying Xiang(项林英), and Guanrong Chen(陈关荣)
Chin. Phys. B, 2023, 32 (**6**): 060502. DOI: 10.1088/1674-1056/acc44e

A novel fractional-order hyperchaotic complex system and its synchronization

Mengxin Jin(金孟鑫), Kehui Sun(孙克辉), and Shaobo He(贺少波)
Chin. Phys. B, 2023, 32 (**6**): 060501. DOI: 10.1088/1674-1056/acc0f6

Diffusive field coupling-induced synchronization between neural circuits under energy balance

Ya Wang(王亚), Guoping Sun(孙国平), and Guodong Ren(任国栋)
Chin. Phys. B, 2023, 32 (**4**): 040504. DOI: 10.1088/1674-1056/ac7bff

Influence of coupling asymmetry on signal amplification in a three-node motif

Xiaoming Liang(梁晓明), Chao Fang(方超), Xiyun Zhang(张希昀), and Huaping Lü(吕华平)
Chin. Phys. B, 2023, 32 (**1**): 010504. DOI: 10.1088/1674-1056/ac9363

Effect of astrocyte on synchronization of thermosensitive neuron-astrocyte minimum system

Yi-Xuan Shan(单仪萱), Hui-Lan Yang(杨惠兰), Hong-Bin Wang(王宏斌), Shuai Zhang(张帅), Ying Li(李颖), and Gui-Zhi Xu(徐桂芝)
Chin. Phys. B, 2022, 31 (**8**): 080507. DOI: 10.1088/1674-1056/ac490c

---

RAPID COMMUNICATION

Stability and multistability of synchronization in networks of coupled phase oscillators

Yun Zhai(翟云)[1,2,3], Xuan Wang(王璇)[2,3], Jinghua Xiao(肖井华)[1], and Zhigang Zheng(郑志刚)[2,3,†]

[1] *School of Science, Beijing University of Posts and Telecommunications, Beijing* 100876, *China*
[2] *Institute of Systems Science, Huaqiao University, Xiamen* 361021, *China*
[3] *College of Information Science and Engineering, Huaqiao University, Xiamen* 361021, *China*

(Received 13 February 2023; revised manuscript received 1 March 2023; accepted manuscript online 28 March 2023)

Coupled phase oscillators usually achieve synchronization as the coupling strength among oscillators is increased beyond a critical value. The stability of synchronous state remains an open issue. In this paper, we study the stability of the synchronous state in coupled phase oscillators. It is found that numerical integration of differential equations of coupled phase oscillators with a finite time step may induce desynchronization at strong couplings. The mechanism behind this instability is that numerical accumulated errors in simulations may trigger the loss of stability of the synchronous state. Desynchronization critical couplings are found to increase and diverge as a power law with decreasing the integral time step. Theoretical analysis supports the local stability of the synchronized state. Globally the emergence of synchronous state depends on the initial conditions. Other metastable ordered states such as twisted states can coexist with the synchronous mode. These twisted states keep locally stable on a sparse network but lose their stability when the network becomes dense.

Keywords: synchronization, coupled phase oscillators, complex networks, multistability

PACS: 05.45.Xt, 05.45.Ra **DOI:** 10.1088/1674-1056/acc808

1. Introduction

Self organization and collective behaviors can be extensively observed in complex systems composed of large numbers of interacting units.[1] Synchronization is a collective emergent behavior ubiquitously observed in many systems,[2,3] such as cardiac pacemaker cells,[4] fireflies,[5] biochemical systems,[6] and neuronal networks.[7] Furthermore, synchronization also has practical significance in aspects of modern life, such as the functioning of power grids which is based on the synchronization of power generators.[8]

Starting from Winfree[9] and Kuramoto,[10] coupled phase oscillators such as the Kuramoto model[11,12] have been adopted as prototype models in exploring synchronization behaviors ubiquitously existing in various backgrounds. Recent developments in network sciences[13,14] emphasize the fundamental significance of synchronization dynamics in complex systems.[15–18]

It is usually approved that stronger coupling makes a higher degree of synchrony among oscillators. Nevertheless, the stability of synchronous states is a subtle issue that needs careful inspection. Recently Zhang *et al.* studied the synchronization of Kuramoto oscillators on small-world networks[19] and found that oscillators may synchronize to each other when the coupling strength exceeds a critical value, and a striking loss of synchrony may happen when the coupling is strong enough. A manifestation of this decoherence is the decrease of the order parameter with increasing the coupling strength.

In this paper, we point out that the desynchronization transition of coupled phase oscillators on networks at strong couplings is not true. We perform numerical simulation for different integral time steps on different networks. It is found that for a given time step, both synchronization and desynchronization occur at $K \geq K_c$ and $K \geq K_d \gg K_c$, respectively, which are manifested by both frequency locking/unlocking and phase coherence/decoherence. The desynchronization threshold significantly increases and diverges with decreasing the integral step. This indicates that the synchronous state can keep stable for strong couplings. Our theoretical discussion on the synchronous state verifies its stability. Meanwhile, theoretical analysis also indicates the possibility of the existence of other metastable ordered state. We find the coexistence of a typical twisted-phase state with the in-phase coherent state. Though twisted states are also ordered states, their order parameters decrease to zero with increasing the coupling. This tendency resembles the incoherent state. Our results also imply that the order parameter is not always a reliable quantity in evaluating the orderness of synchrony in coupled phase oscillators.

This paper is arranged as follows. In Section 2, we introduce the Kuramoto model on general networks and some necessary quantities in describing the collective dynamics of coupled oscillators. Then in Section 3, we perform numerical studies of Kuramoto oscillators on different network topologies for different integral time steps. We discuss the impact of the integral step on desynchronization of networks of cou-

[†]Corresponding author. E-mail: zgzheng@bnu.edu.cn

© 2023 Chinese Physical Society and IOP Publishing Ltd

pled phase oscillators. In Section 4, we discuss the stability of the synchronous state in coupled phase oscillators in terms of linear stability analysis and potential function analysis. We then study the possibility of multistability at the onset of synchronization in Section 5. Particularly, we find that the twisted state is a typical metastable ordered state that can coexist with synchrony. A concluding remark is given in Section 5.

2. Modeling networks of coupled phase oscillators

By considering a general topology of mutual interactions among oscillators, one supposes a system of N oscillators with phases and nature frequencies $\{\theta_i(t), \omega_i\}$, $i = 1, 2, \ldots, N$. The Kuramoto-type model describes coupled phase dynamics and can be written as

$$\dot{\theta}_i = \omega_i + \frac{K}{k_i + 1} \sum_{j=1}^{N} A_{ij} \sin(\theta_j - \theta_i), \tag{1}$$

where $i = 1, 2, \ldots, N$, and K is the coupling strength among the oscillators. The coupling network topology is described by the symmetric adjacency matrix $\boldsymbol{A} = (A_{ij}), i, j = 1, 2, \ldots, N$, where $A_{ij} = A_{ji} = 1$ if oscillators i and j are coupled to each other, and $A_{ij} = A_{ji} = 0$ otherwise. The degree of the i-th node can be computed from the adjacency matrix as $k_i = \sum_{j=1}^{N} A_{ij}$.

The collective behavior of coupled oscillators on different networks is conveniently characterized by the following complex order parameter:

$$z(t) = R(t)\, \mathrm{e}^{\mathrm{i}\psi(t)} \equiv \frac{1}{N} \sum_{j=1}^{N} \mathrm{e}^{\mathrm{i}\theta_j(t)}, \tag{2}$$

where i is the imaginary unit, $R(t)$ and $\psi(t)$ describe the coherence factor and collective phase, respectively. In the limit $N \to \infty$, $R = 0$ represents an incoherent state with phases of oscillators homogeneously distributed in $[0, 2\pi)$. $R > 0$ implies some degree of synchrony among oscillators, and $R = 1$ means a fully in-phase synchronous state.

One may also introduce the following function to measure the degree of frequency locking:

$$\Delta\Omega = \frac{1}{N} \sum_{j=1}^{N} \left| \Omega_j - \omega_0 \right|, \tag{3}$$

where Ω_j is the time-averaged frequency of the j-th oscillator defined as

$$\Omega_j = \left\langle \dot{\theta}_j \right\rangle \equiv \lim_{T \to \infty} \frac{1}{T} \int_{t_0}^{t_0 + T} \dot{\theta}_j(t)\, \mathrm{d}t, \tag{4}$$

and ω_0 is the mean natural frequency of the system

$$\omega_0 = \frac{1}{N} \sum_{j=1}^{N} \omega_j. \tag{5}$$

All oscillators are frequency locked when $\Delta\Omega = 0$. If one wishes to know the detailed information of the synchronization dynamics, the synchronization bifurcation tree $\{\Omega_i(K), i = 1, 2, \ldots, N\}$ can be introduced[20–22] to study the detailed information of locking processes among oscillators by increasing the coupling strength K.

There have been extensive theoretical studies on the synchronization behaviors of the model (1).[11] For the fully connected network case, i.e., $k_i = N - 1$, Eq. (1) describes the dynamics of the traditional mean-field Kuramoto model. In the thermodynamics limit $N \to \infty$, statistical description can be introduced to study the collective behavior of Eq. (1).

Kuramoto[23] proposed the self-consistency approach to analytically predict the transition from incoherence to synchronization. It was found that synchrony among oscillators emerges when the coupling strength exceeds the critical value $K_c = 2/\pi g(\omega_0)$, i.e., $R = 0$ for $K < K_c$, and $R > 0$ as $K > K_c$. Here $g(\omega)$ is the distribution of the intrinsic frequency.

The synchronization transition has been extensively investigated, and the mechanism of the emergence of synchrony was revealed in terms of microscopic synchronization bifurcation tree,[20–22] statistical self-consistency approach,[11,23] dynamical Watanabe–Strogatz transformation[24–26] and the macroscopic Ott–Antonsen ansatz.[27,28]

In the following discussion, we will perform numerical simulations of system (1) for different network topologies to check the influence of network topology synchronization. Here we mainly focus on nearest-neighbor regular (NNR) networks, Erdos–Renyi (ER) random networks, small-world (SW) networks, and scale-free (SF) networks.[14] For an NNR network, the adjacency matrix satisfies $A_{i,i\pm j} = 1$ for $j \le L$ and $A_{i,i\pm j} = 0$ for $j > L$, where L is the neighbor distance. The degree $k_i = 2L$ for an NNR network. An ER network can be constructed by setting a linking probability p for a pair of nodes. The SW network can be generated using the Watts–Strogatz rewiring algorithm,[29] by randomly removing some regular edges from an NNR network and randomly adding the same number of long-distance edges. The scale-free network can be generated by using the Barabasi–Albert preferential growth algorithm,[30] i.e., starting from the initial m_0 nodes and adding a node with m new edges at each step following the preferential probability $p_i = k_i/(\sum_i k_i)$.

Throughout the numerical simulations, natural frequencies $\{\omega_i\}$ of oscillators are randomly chosen from the uniform distribution

$$g(\omega) = \frac{1}{2\gamma} \quad \text{for} \quad \omega \in [-\gamma, \gamma]. \tag{6}$$

In our simulations, the parameter $\gamma = 1/2$.

The equations of motion are numerically integrated in terms of the fourth-order Runge–Kutta algorithm. In order to examine the accuracy and error accumulations brought by

the discreteness of numerical iterations, one chooses different time steps Δt ranging from relatively large to very small ones. The initial states of oscillators $\{\theta_i(0)\}$ are randomly chosen from the interval $[0, 2\pi)$.

3. Synchronization–desynchronization transitions: integral step matters

We first study the synchronization dynamics of Kuramoto oscillators on the ER network with the connection probability $p = 0.5$, the SW network with the average degree $\langle k \rangle = 10$, and the SF network with $\langle k \rangle = 9.2$, respectively. The number of nodes of all these networks is set to be $N = 300$. We compute the frequency difference $\Delta\Omega$ defined by Eq. (3) and the order parameter R defined by Eq. (2) to investigate the synchronization dynamics of coupled phase oscillators described by Eq. (1) for the ER, SW, and SF network topologies, respectively.

In Fig. 1, synchronization properties of Kuramoto oscillators on three types of networks are presented, where the frequency difference Δ and the order parameter $\langle R \rangle$ versus the coupling strength K are plotted. The integral time step $\Delta t = 0.1$. In Fig. 1(a), for the case of the SW network, the $\Delta\Omega \sim K$ curve shows that there exists a critical $K_c^{SW} \approx 0.9$, when $K < K_c^{SW}$, $\Delta\Omega \neq 0$. While as $K > K_c^{SW}$, $\Delta\Omega = 0$ keeps with increasing the coupling strength. The critical coupling K_c^{SW} corresponds to a transition from the asynchronous state to the global locking state. A good coincidence between global phase locking and the phase coherence can be found in Fig. 1(b), where the order parameter R increases sharply from a small value $R \sim 1/N$ at $K = K_c^{SW}$, implying that the oscillators are phase coherent when $K > K_c^{SW}$. With further increasing the coupling strength, it can be found that R increases to nearly full synchrony $R = 1$, and the frequency locking $\Delta\Omega = 0$ is always kept. This means that the in-phase synchronous state is maintained in a very large coupling regime.

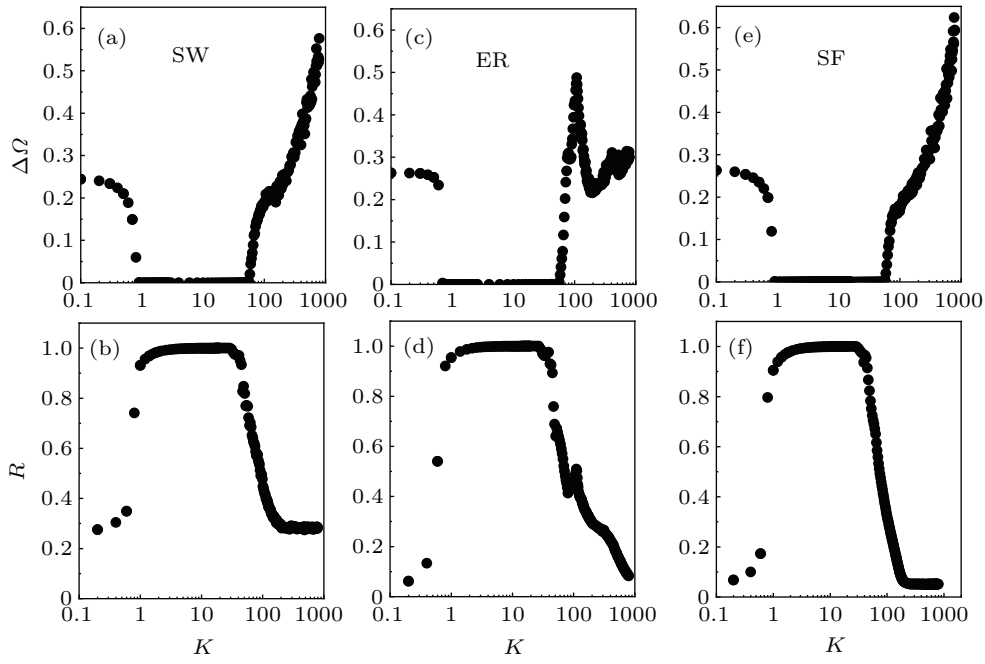


Fig. 1. Synchronization dynamics of coupled phase oscillators with different network topologies for the integral time step $\Delta t = 0.1$. (a)–(c) The frequency difference $\Delta\Omega$ varying with the coupling strength K for ER random network, SW network, and SF network, respectively. (d)–(f) The order parameter R versus the coupling strength for networks corresponding to (a)–(c). The number of oscillators $N = 300$.

However, the synchrony tendency breaks down when the coupling strength is increased above the second threshold $K_d^{SW} \approx 56.0$. It can be seen from Fig. 1(a) that $\Delta\Omega$ becomes non-zero as $K > K_d^{SW}$, meaning a loss of global frequency locking. Meanwhile, R decreases with further increasing the coupling (see Fig. 1(b)), indicating a deteriorated phase coherence of oscillators at strong couplings.

The above desynchronization transition reproduced the results proposed by Zhang *et al.*[19] They studied the synchronization of Kuramoto oscillators on SW networks and found that oscillators may synchronize to each other at a small coupling while a striking loss of synchrony happens when the coupling exceeds a very large critical strength. This asynchrony is manifested as the decrease of order parameter R with increasing the coupling.

Here we can find that similar synchronization–desynchronization transitions can occur not only in SW networks, but also in ER and SF networks, as shown in Figs. 1(c), 1(d) and 1(e), 1(f), respectively. The difference between these networks is the value of critical couplings, i.e., $K_c^{ER} \approx 0.7$, $K_c^{SF} \approx 0.9$, $K_d^{ER} \approx 56$, and $K_d^{SF} \approx 57$. This indicates that the synchronization–desynchronization transition takes place irrelevant of network topologies. On the other hand, the transition at K_d is beyond our intuition. Is this transition true? If so,

what is the mechanism responsible for this desynchronization transition?

To check the above observation, in Fig. 2, we further compute the order parameter R and the difference $\Delta\Omega$ against the coupling K by integrating Eq. (1) for a smaller time step $\Delta t = 10^{-2}$. It is shown that the critical coupling for the synchronization transition at $K \geq K_c$ can still be found, and the values of K_c are almost the same as those in Fig. 1 for a larger time step $\Delta t = 10^{-1}$, where $K_c^{SW} \approx 0.8$, $K_c^{ER} \approx 0.7$, and $K_c^{SF} \approx 0.9$. This indicates that the intrinsic property of synchronization transition is independent of the numerical algorithm and the integral step. As a common sense, this independence should also be valid for the desynchronization transition, i.e., the critical coupling K_d should not change drastically by changing integration step Δt. However, the desynchronization transition takes place at much larger critical couplings, as shown in Fig. 2, where $K_d^{SW} \approx 450$ (Figs. 2(a) and 2(b)), $K_d^{ER} \approx 540$ (Figs. 2(c) and 2(d)), and $K_d^{SF} \approx 550$ (Figs. 2(e) and 2(f)), respectively.

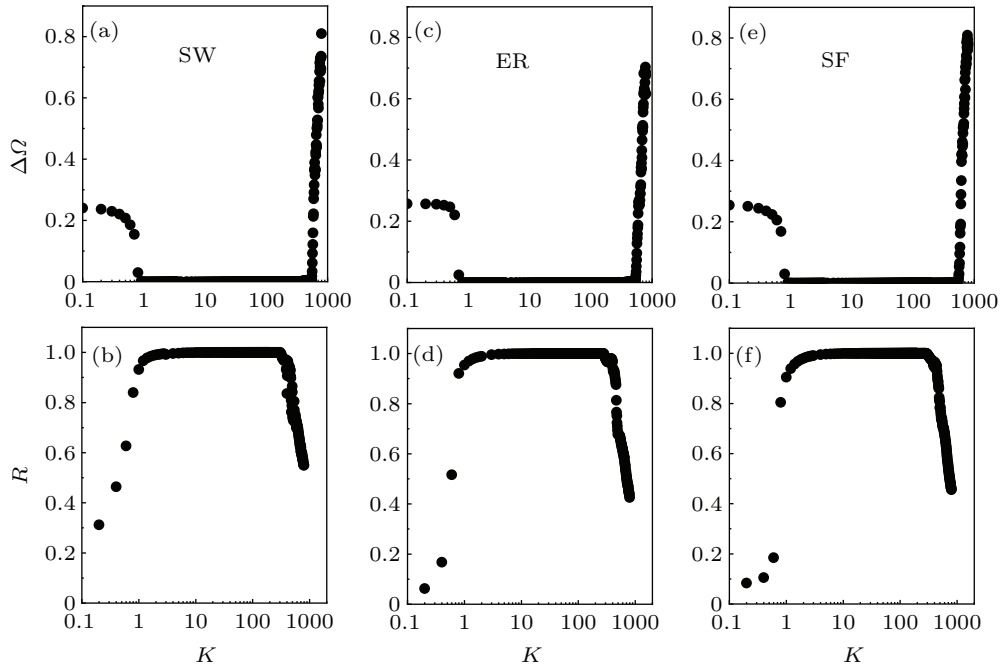


Fig. 2. Synchronization dynamics of $N = 300$ coupled phase oscillators with the same network topologies as in Fig. 1 for the integral time step $\Delta t = 0.01$. (a)–(c) The frequency difference $\Delta\Omega$ varying with the coupling strength K. (d)–(f) The order parameter R versus the coupling strength for networks corresponding to (a)–(c).

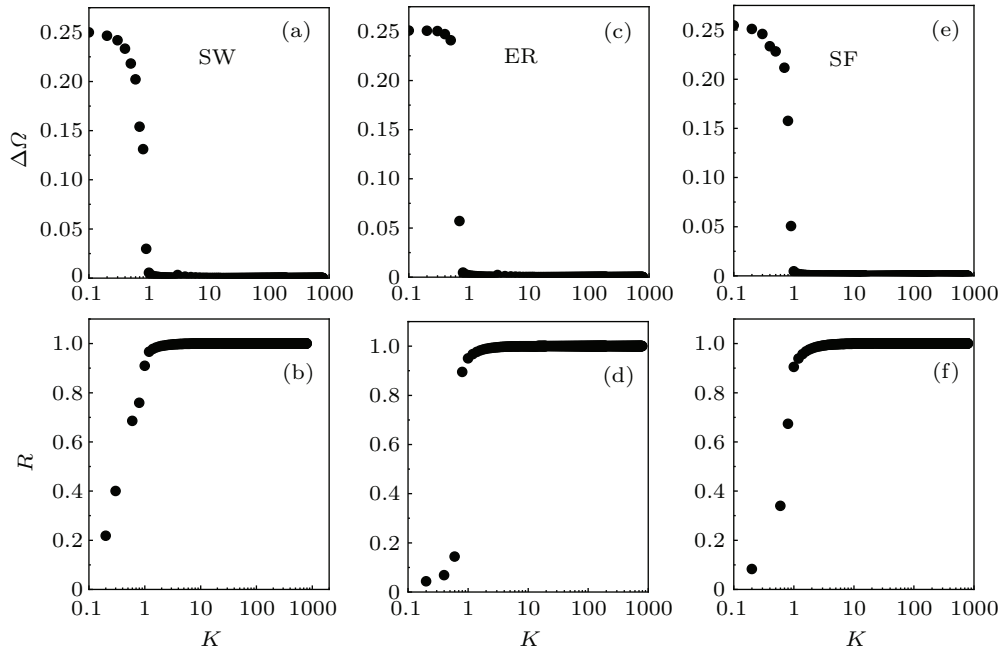


Fig. 3. Synchronization dynamics of $N = 300$ coupled phase oscillators with the same network topologies as in Fig. 1 for the integral step $\Delta t = 10^{-3}$. (a)–(c) The frequency difference $\Delta\Omega$ varying with the coupling strength K. (d)–(f) The order parameter R versus the coupling strength for networks corresponding to (a)–(c).

We further check the above phenomena by computing the same quantities of coupled oscillators with the same parameters but for a smaller integral step $\Delta t = 10^{-3}$. As shown in Fig. 3, the first transition thresholds K_c from incoherence to synchronization for different networks are $K_c^{SW} \approx 0.9$, $K_c^{ER} \approx 0.8$, and $K_c^{SF} \approx 1.0$, i.e., K_c remains unchanged for all three types of network topologies. On the other hand, the second thresholds K_d of the desynchronization transition cannot be seen in the coupling regime shown in Fig. 3. Further computation for $\Delta t = 10^{-3}$ at larger coupling regimes gives the thresholds $K_d^{SW} \approx 2810$, $K_d^{ER} \approx 2980$, and $K_d^{SF} \approx 2870$.

The two critical couplings K_c and K_d against the time step Δt are summarized in Fig. 4. Each transition point K_c or K_d is determined by increasing and scanning the coupling strength K from 0. It can be seen that the synchronization critical coupling K_c remains almost unchanged by varying the integral time step Δt, while the desynchronization critical coupling K_d exhibits a divergence with decreasing the time step Δt in approximately a power law

$$K_d \propto \Delta t^{-\alpha}, \tag{7}$$

where the exponent $\alpha \approx 0.84$. Moreover, the network topology does not remarkably affect the critical coupling K_d.

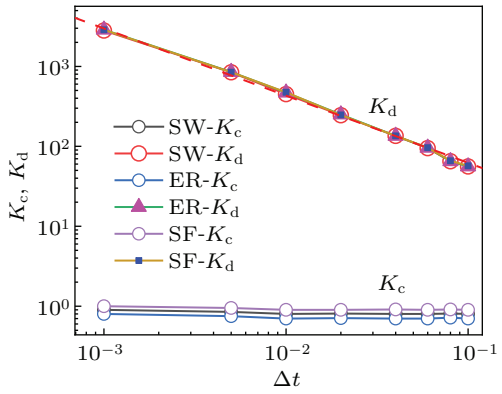


Fig. 4. The critical couplings K_c and K_d for different integral steps Δt for ER, SW, and SF networks.

We also test the effect of natural-frequency distribution $g(\omega)$ and the number of oscillators N, our simulations indicate that K_d is also irrelevant to these factors. These tokens indicate that K_d is only related to the discretization during the numerical integrations of Eq. (1), i.e., the second transition is an artifact of numerical simulation.

The above results strongly support the conclusion that the synchronous state remains stable as long as the coupling $K \geq K_c$. However, by increasing the accuracy of integral of dynamical equations, $K_d \to \infty$, i.e., the second transition to desynchronization does not exist. Therefore we make a judgement that the previous results of desynchronization at strong coupling[19] are incorrect. This gives us a kind reminder that the integration step is very important in performing numerical algorithms to solve differential equations.

Numerical computation of the integration of variable-continuous differential equations is essentially a discretizing process, and this may definitely produce various errors with change from time-continuous evolution to discrete iterations. Both the discretization algorithm and the integration step are important in influencing the accuracy of numerical simulations. Different discretization algorithms will always introduce different degrees of truncation errors, and a finite integral step may bring out accumulated errors.

In principle, a small enough step is the best choice to suppress the computational error. However, practical computations require a tradeoff between computational cost and benefit. Therefore the integral step is usually chosen as an appropriate and optimal value. For equations of coupled phase oscillators, e.g., the Kuramoto-like system (1), a choice of time step $\Delta t = 10^{-2}$ is fine to give reliable results, and even a larger step $\Delta t = 10^{-1}$ also seems to produce reasonable data. However, the values of system parameters should be carefully taken into account. Our simulations indicate that there exists a risk during the exploration of dynamics at strong couplings. If the integral step is not small enough, the error brought by numerical discreteness of the integral may lead to incorrect results, and even leads to the instability.

4. Stability of the synchronous state

Let us theoretically analyze the stability of the synchronous state of system (1). A typical synchronous state is the in-phase state (IPS) defined as

$$\theta_1(t) = \theta_2(t) = \cdots = \theta_N(t) = s(t). \tag{8}$$

An IPS has the maximum coherence factor $R = 1$. However, it should be noted that the IPS (8) is not the solution of the system (1) with natural-frequency mismatches unless $K \to \infty$. When $K \gg K_c$, all oscillators are frequency synchronized, and ω_i in Eq. (1) can be omitted, then one has

$$\dot{\theta}_i \approx \frac{K}{k_i + 1} \sum_{j=1}^{N} A_{ij} \sin(\theta_j - \theta_i). \tag{9}$$

The IPS is the natural solution of Eq. (9). Consider a small deviation of the phases from the synchronous solution $\theta_i(t) = s(t) + \delta\theta_i(t)$. By linearizing Eq. (9) around the synchronous manifold $s(t)$, one obtains the linearized equations

$$\delta\dot{\theta}_i = \frac{K}{k_i + 1} \sum_{j=1}^{N} A_{ij}(\delta\theta_j - \delta\theta_i). \tag{10}$$

For a regular network, $k_i = k$, Eq. (10) can be written in the following vector form:

$$\delta\dot{\boldsymbol{\theta}} = \frac{K}{k+1}(\boldsymbol{A} - k\boldsymbol{I})\delta\boldsymbol{\theta} = \frac{K}{k+1}\boldsymbol{L}\delta\boldsymbol{\theta}, \tag{11}$$

where $\delta\boldsymbol{\theta} = (\delta\theta_1, \delta\theta_2, \ldots, \delta\theta_N)^{\mathrm{T}}$, $\boldsymbol{A}$ is the adjacency matrix, and $\boldsymbol{I}$ is the $N \times N$ identity matrix. The second term comes from $k_i = \sum_{j=1}^{N} A_{ij}$. Here $\boldsymbol{L}$ is just the Laplacian matrix, where

the largest eigenvalue $\lambda_1 \leq 0$. Therefore the IPS $\theta_i = s(t)$ $(i = 1,2,\ldots,N)$ is stable when $K > K_c$.

The above analysis is based on a linear stability scheme and implies a local stability of the IPS. In fact, both Eqs. (1) and (9) correspond to gradient systems. For example, for Eq. (1), one may introduce the following potential function:

$$V(\{\theta_i\}) = -\sum_{i=1}^{N}\omega_i\theta_i + \frac{K}{2}\sum_{i=1}^{N}\frac{1}{k_i+1} \times \sum_{j=1}^{N}A_{ij}\left[1-\cos(\theta_i-\theta_j)\right], \tag{12}$$

by which Eq. (1) can be written as

$$\dot{\theta}_i = -\frac{\partial V(\{\theta_j\})}{\partial\theta_i}. \tag{13}$$

Because

$$\frac{\mathrm{d}V}{\mathrm{d}t} = \sum_{i=1}^{N}\frac{\partial V}{\partial\theta_i}\dot{\theta}_i = -\sum_{i=1}^{N}\left(\frac{\partial V}{\partial\theta_i}\right)^2 \leq 0, \tag{14}$$

system (1) will evolve towards the direction of a minimum potential $V_{\min}$. When $\partial V/\partial\theta_i = 0$ for $i = 1,2,\ldots,N$, the system is at its equilibrium state.

A natural equilibrium state is the IPS $s(t)$, which is the minimum $V_{\min} = 0$ satisfying the condition $\mathrm{d}V/\mathrm{d}t = 0$ and the stable ordered state. Although the discussion above is shown for regular networks, this conclusion should be irrelevant to the network topology.

5. Coexisting metastable modes: twisted states

As shown in the above discussion, as long as the potential function satisfies the gradient condition $\mathrm{d}V/\mathrm{d}t \leq 0$, the system will evolve to a stationary state with $\mathrm{d}V/\mathrm{d}t = 0$. In fact, the IPS $s(t)$ is a globally minimum-potential and the most stable stationary state. Apart from the IPS, the following phase configuration also satisfies the requirement of $\mathrm{d}V/\mathrm{d}t = 0$:

$$\theta_i(t) = \omega t + \frac{2\pi m}{N}i + \theta_0, \quad i = 1,2,\ldots,N, \tag{15}$$

where m is an integer, and θ_0 is a constant depending on the initial condition. This state is called the m-twisted state (TS), and m is the winding number.

Obviously when the winding number m is an integer multiplication of N, i.e., $m = Nm_0$ with m_0 being an integer, $\theta_i - \theta_j = 2\pi m_0(i-j)$, i.e., the TS goes back to the IPS. On the other hand, when $m \neq 0$ and $m \neq Nm_0$, the phases of oscillators distribute evenly by a constant phase shift $2\pi m/N$. In this case, it is easily found that the order parameter $R(t) = 0$, which occurs also for an incoherent state. This is distinctly different from the IPS that satisfies $R(t) = 1$.

Although the coherence factor $R = 0$, a twisted state is still an ordered state. For the system (9), oscillators are identical. For this case, an arbitrarily small coupling may induce ordered TS states. The stability of TS depends on both the coupling distance (degree) and the winding number. This topic has been extensively studied in recent years.[31–35] However, if there exists heterogeneity in natural frequencies of oscillators, it is possible that the phase oscillators may still possess the TS when the coupling is increased beyond a critical value of achieve global frequency locking. It is thus very interesting to study the emergence of TS and its dependence on the coupling in detail.

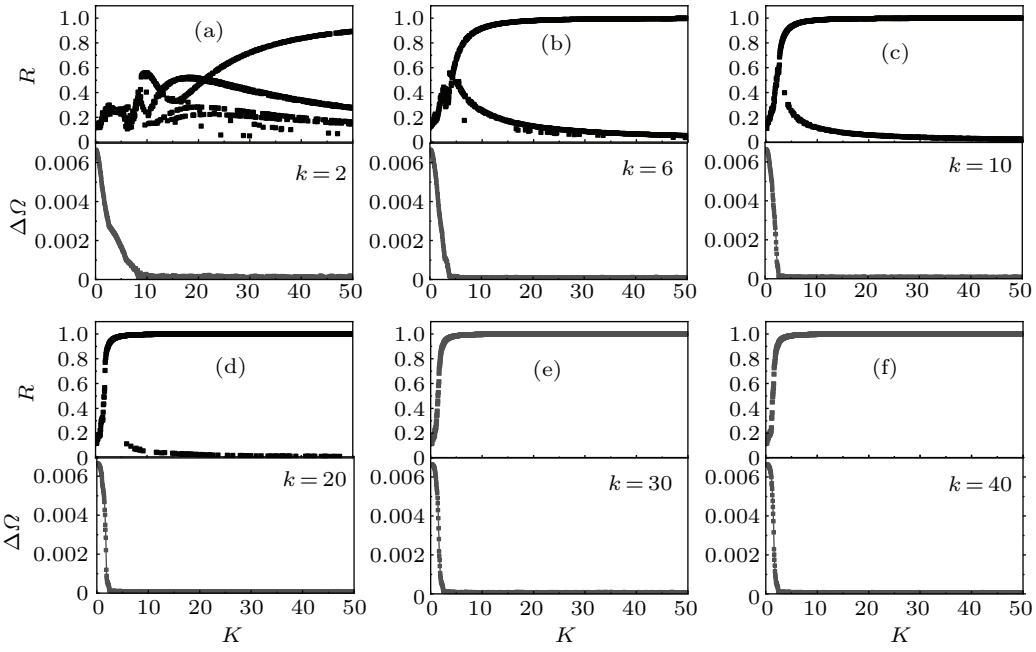


Fig. 5. Multistable dynamics of $N = 50$ coupled phase oscillators with NNR topologies. Natural frequencies obey the uniform difstribution given in Eq. (6). Random initial conditions are adopted at every given coupling strength during the simulation. From (a)–(f), the degrees of the networks are $k = 2$, 6, 10,20, 30, and 40, respectively. In each sub-figure, the upper one is the order parameter R versus the coupling K, and the lower one is the frequency difference Δ against the coupling K.

In Fig. 5, we study the collective dynamics of the nearest-neighbor coupled phase oscillator systems (1) with different degrees by scanning the variation of the averaged order parameter R defined by Eq. (2) and the frequency difference $\Delta\Omega$ defined by Eq. (3) against the coupling K. Random initial conditions at each coupling strength K are adopted, i.e., θ_i are randomly chosen in the interval $[0, 2\pi]$. Oscillator number are set as $N = 50$. The natural frequencies ω_i are randomly chosen according to the uniform distribution $g(\omega)$ given by Eq. (6). In Fig. 5(a), R varying against the coupling strength K is shown in the upper part, where the degree $k = 2$ (the ring network). As a comparison to better understand what happens for different couplings, the difference $\Delta\Omega$ is also plotted in the lower part of Fig. 5(a). It can be found that R varies erratically against the coupling strength when $K < K_c$. When the coupling $K \geq K_c$, several branches of the order parameter can be observed. The emergence of multiple branches comes from random initial states, implying the local stability of different collective dynamics. The most robust branch that $R \to 1$ for large K is the IPS, which increases with increasing the coupling strength. One interesting observation is that there exist other multiple R–K branches with each branch decreasing with increasing the coupling strength. The tendency of these branches is similar to the decreasing R found in Figs. 1 and 2 for $K > K_d$. However, these two seemingly decreasing tendencies are completely different. The decreasing R curves in Figs. 1 and 2 are due to the loss of synchrony. In the present case, oscillators are still synchronized, which can be shown from the lower subfigure that $\Delta = 0$ for $K > K_c$. One anticipates that for all these branches $R \to 0$ as $K \to \infty$.

We also compute the collective properties of coupled oscillators on NNR networks with larger degrees k in Figs. 5(b)–5(f) for the degrees $k = 6$, 10, 20, 30, and 40, respectively. In all the lower sub-figures, the variation of the frequency difference Δ with the coupling gives the critical coupling for global synchronization. One may easily find that for low degrees such as $k = 6$, 10, and 20, multiple branches of the order parameter R coexist, implying the multistability of synchronous states with different phase patterns. On the other hand, the number of branches decreases with increasing the degree k of nodes. When the network connection becomes dense enough, as shown in Figs. 5(e) and 5(f), only the IPS is left, and the decreasing R branch disappears. This means that those low-R states become unstable in a dense network.

It is important to identify the collective topologies $\{\theta_i\}$ of these low-R states. In these regimes, frequency synchronization is still maintained, hence a phase-disordered topology should be excluded. For ideal twisted states expressed by Eq. (15) with $m \neq 0$ in coupled identical phase oscillators, one has the order parameter $R = 0$. For non-identical oscillators with distributed natural frequencies, one does not expect a strict $R = 0$, but those low-R states are very probably related to ideal twisted states. To verify this conjecture, in Fig. 6, we study the order-parameter dynamics by plotting R versus the coupling strength K. For all curves, at each given value of the coupling K, one starts from different initial m-twisted configurations

$$\theta_i^{(0)} = \frac{2\pi m}{N} i, \quad i = 1, 2, \ldots, N.$$

We give the R–K curves for initial-configuration winding numbers $m = 1$, 2, 3, 4, 5, 15 and 25, respectively. The regular network contains $N = 50$ oscillators with the degree $k = 2$. It is clearly shown that as $K < K_c$, the system is in the asynchronous state, and the R–K relation is independent of various initial configurations $\{\theta_i^{(0)}\}$. On the other hand, when the coupling is larger than the synchronous threshold, i.e., $K > K_c$, these curves bifurcate into multiple branches. For branches starting from initial configurations with low winding numbers (see $m = 1$–10), the curves exhibit a decreasing tendency with increasing the coupling. When m is very large, for example $m = 15$ and 25, as shown in Fig. 6, the order parameter R exhibits a normal increasing relation when the coupling strength is large enough.

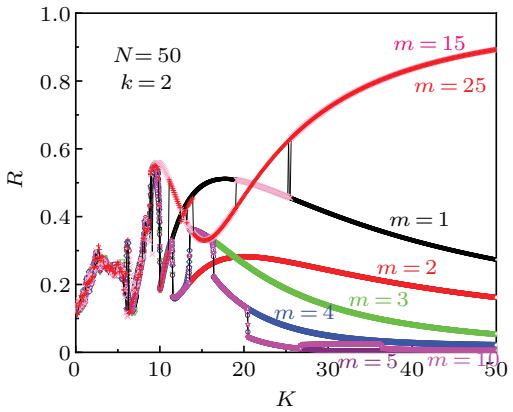


Fig. 6. The order parameter R varying against the coupling for $N = 50$ coupled phase oscillators for NNR network with $k = 2$. Different colored R–K curves are plotted for different initial twisted states with $m = 1$, 2, 3, 4, 5, 10, 15, and 25, respectively. For initial configurations with small winding numbers, R decreases with increasing the coupling (see $m = 1$–10). As m becomes larger, R increases normally with increasing the coupling (see $m = 15$ and 25). The R–K curve for $m = 10$ exhibits multiple jumps between different branches.

It is interesting to examine the long-time configuration $\{\theta_i^{t\to\infty}\}$ of the R–K curves presented in Fig. 6. By starting from different initial slightly-perturbed TS configurations $\{\theta_i^0 = 2\pi m/N\}$ with winding numbers $m = 1$, 3, 5, 7 shown as blue solid lines in Fig. 7, the long-time configurations $\{\theta_i^\infty\}$ for different degrees $k = 2$, 10, 20, 40 are shown as red dots, where θ_i is set as 2π modulus. The number of sawteeth corresponds to the winding number m. For the sparse-connection case $k = 2$, as seen from column (a), all the initial twisted configurations $m = 1$, 3, 5, 7 are persisted during the evolution, i.e., the long-time configurations can remain their initial

preparations. This indicates that most of the twisted modes are stable. When the degree becomes larger, e.g., $k = 10$, as shown in column (b) of Fig. 7, only low-m mode keeps stable, and a bit higher m modes will become unstable and replaced by the IPS ($m = 0$). Similar scenarios can be observed for the cases of $k = 20$ (column (c)) and $k = 40$ (column (d)).

The above discussion indicates that when the coupling strength becomes large, not only the in-phase mode corresponding to an increasing $R(K)$ emerges, but also the twisted modes with a decreasing $R(K)$ bifurcate and coexist with the in-phase mode. This gives an interesting behavior that is much different from the cases given by Figs. 1–3.

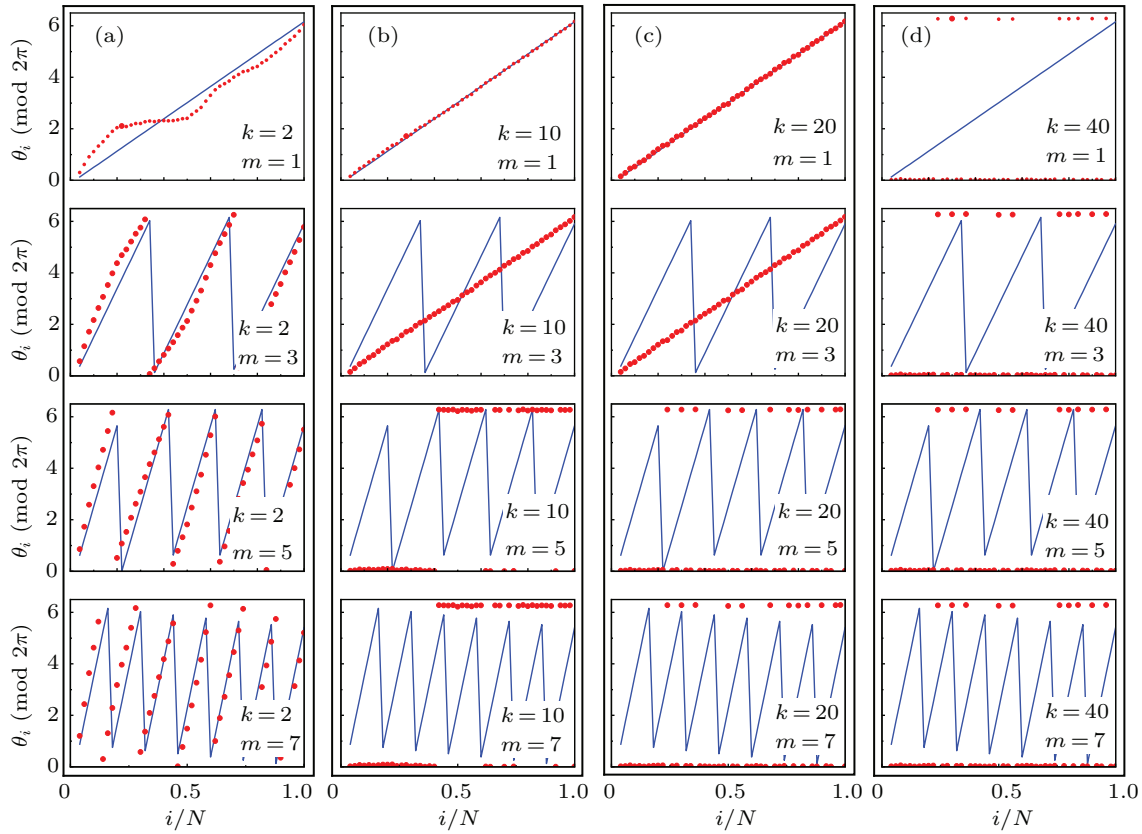


Fig. 7. The long-time configurations of $N = 50$ coupled oscillators for different degrees $k = 2$, 10, 20, 40 corresponding to columns (a), (b), (c), (d), respectively. For each column, from up to down, the system evolves starting from the initial twisted states with $m = 1$, 3, 5, and 7, respectively. The coupling strength $K = 50$. Initial twisted-state configurations are given by solid lines, and the long-time configurations are plotted as dots. The 2π module is performed for the phase variables θ_i, and the number of segments corresponds to the winding number m.

6. Concluding remarks

In this paper, we focus on the synchronization dynamics of coupled phase oscillators. We first focus on the stability of synchronous state. The investigation of the influence of integral steps indicates that it is important to choose a proper integral step in numerical simulations of time-continuous dynamical systems. An appropriate integration algorithm and a suitable step can ensure the convergence and safety of numerical simulation, while a finite integral step may bring false data and the instability of synchrony states. By extensive numerical simulations, we point out that the desynchronization at strong couplings is a purely artificial consequence of numerical simulation. We find that the desynchronization transition point $K_{\rm d}$ increases with decreasing time step Δt in a power law.

Though the synchronous state is stable at strong couplings, the numerical-integral-induced instablity of synchronous state we proposed in this paper reminds us the possibility of desynchronization in coupled phase maps. We recently studied the coupled circle maps and found the synchronization–desynchronization transitions. This is another interesting topic that is discussed elsewhere.[36]

We theoretically discuss the stability of the synchronous state and verify that the in-phase state keeps locally stable for strong couplings. Moreover, multistability in phase space implies the existence of other metastable states that may coexist with the IPS in the synchronous regime. A typical metastable state is the twisted state. Different from the IPS that has the strongest phase coherence $R = 1$, an TS is also the frequency-locking state, but the phases distribute with finite phase shifts as twisted waves, resulting in $R = 0$. Our study indicates that multiple TS's can be stable and coexist with the IPS for sparse networks. When the network becomes dense enough, the TS's ($m \neq 0$) will lose their stability, and only the IPS is left.

The coupling function is also a key ingredient in determining the synchronization property of coupled oscillators. General discussions of synchronization on networks in

terms of the master-stability function approach[37] indicate that there are three types of synchrony routes by varying the coupling strength depending on the coupling schemes. We believe it is possible to construct other types of coupling functions rather than the simple sinusoidal function to explore synchronization–desynchronization transitions.

Acknowledgement

Project supported by the National Natural Science Foundation of China (Grant No. 11875135).

References

[1] Zheng Z G 2021 *An introduction to emergence dynamics in complex systems* (Singapore: Springer Singapore) pp. 133–196
[2] Pikovsky A, Rosenblum M and Kurths J 2001 *Synchronization: a universal concept in nonlinear sciences* (Cambridge: Cambridge University Press)
[3] Zheng Z G 2019 *Emergence Dynamics in Complex Systems: From Synchronization to Collective Transport*, vol. 1 (China Science Publishing Media Ltd) (in Chinese)
[4] Osaka M 2017 *Appl. Math. B* **8** 1227
[5] Buck J B and Buck E 1968 *Science* **159** 1319
[6] Kiss I Z, Zhai Y and Hudson J L 2002 *Science* **296** 1676
[7] Chandra S, Hathcock D, Crain K D, Antonsen T M, Girvan M and Ott E 2017 *Chaos* **27** 033102
[8] Witthaut D, Hellmann F, Kurths J, Kettemann S, Meyer-Ortmanns H and Timme M 2022 *Rev. Mod. Phys.* **94** 015005
[9] Winfree A T 1967 *J. Theor. Biol.* **16** 15
[10] Kuramoto Y 1975 in *International Symposium on Mathematical Problems in Theoretical Physics*, edited by Araki H (Berlin, Heidelberg: Springer Berlin Heidelberg) pp. 420–422
[11] Acebron J A, Bonilla L L, Perez Vicente C J, Ritort F and Spigler R 2005 *Rev. Mod. Phys.* **77** 137
[12] Rodrigues F A, Peron T K D M, Ji P and Kurths J 2016 *Physics Reports* **610** 1
[13] Albert R and Barabási A L 2002 *Rev. Mod. Phys.* **74** 47
[14] Dorogovtsev S N and Mendes J F F 2022 *The nature of complex networks* (OUP Oxford)
[15] Wang X F 2002 *Int. J. Bifurc. Chaos* **12** 885
[16] Boccaletti S, Latora V, Moreno Y, Chavez M and Hwang D U 2006 *Physics Reports* **424** 175
[17] Arenas A, Díaz-Guilera A, Kurths J, Moreno Y and Zhou C 2008 *Physics Reports* **469** 93
[18] Boccaletti S, Almendral J A, Guan S, Leyva I, Liu Z, Sendia-Nadal I, Wang Z and Zou Y 2016 *Physics Reports* **660** 1
[19] Zhang Y and Xiao R 2014 *Physica A* **416** 33
[20] Zheng Z G, Hu G and Hu B B 1998 *Phys. Rev. Lett.* **81** 5318
[21] Zheng Z G, Hu B B and Hu G 2000 *Phys. Rev. E* **62** 402
[22] Hu B B and Zheng Z G 2000 *Int. J. Bifurc. Chaos* **10** 2399
[23] Kuramoto Y 1984 *Chemical oscillations, Waves, and Turbulence* (Springer-Verlag)
[24] Watanabe S and Strogatz S H 1993 *Phys. Rev. Lett.* **70** 2391
[25] Watanabe S and Strogatz S H 1994 *Physica D* **74** 197
[26] Marvel S A, Mirollo R and Strogatz S H 2009 *Chaos* **19** 043104
[27] Ott E and Antonsen T M 2008 *Chaos* **18** 037113
[28] Ott E and Antonsen T M 2009 *Chaos* **19** 023117
[29] Watts D J and Strogatz S H 1998 *Nature* **393** 440
[30] Barabási and Albert 1999 *Science* **286** 509
[31] Wiley D A, Strogatz S H and Girvan M 2006 *Chaos* **16** 015103
[32] Zou W and Zhan M 2009 *SIAM J. Appl. Dyn. Syst.* **8** 1324
[33] Xie Y, Zhang L, Guo S J, Dai Q L and Yang J Z 2019 *PLoS ONE* **14** e0213471
[34] Girnyk T, Hasler M and Maistrenko Y L 2012 *Chaos* **22** 013114
[35] Goebel M, Mizuhara M S and Stepanoff S 2021 *Chaos* **31** 103106
[36] Zhai Y, Xiao J H and Zheng Z G 2023 *Chin. Phys. B* **32** 060505
[37] Pecora L M and Carroll T L 1998 *Phys. Rev. Lett.* **80** 2109